

electronics to the sensor. Furthermore, by partially covering the surface with metal, separate pH and redox measurements can be made at each site to control for potentiometric stability of the system if one or the other of these solution parameters is made stable at each site by an appropriate buffer. Another feature of the LAPS that lends convenience to the fabrication of biosensors is its planar surface. The flat polished sensing surface has two significant attributes. First, it is easy to create fluid seals to maintain the aqueous solution only in contact with the insulator surface. For high-sensitivity assays, microscopic fluid leaks between the aqueous compartment and the electrical contact on the back side of the semiconductor can result in substantial potentiometric drifts. For some sensor configurations, a resistive path of 100 gigaohms through the fluid leak into a small volume can result in substantial drifts. Second, the flat surface makes it possible to generate very small, defined aqueous volumes. These volumes can be as small as a nanoliter. The advantage of using small volumes for performing high-sensitivity assays is discussed above. We have detected one attomole (600,000) of enzyme molecules adsorbed to filter paper 100 μm thick. The time required to make this determination was approximately 2 minutes.

The principal advantage of biosensors, such as the one described here, is the ease with which miniaturization can be achieved. This miniaturization in turn facilitates multiplicity and high sensitivity. Specific applications of this methodology to enzyme-linked immunochemical assays for therapeutic drugs, hormones, and bacterial pathogens will be given elsewhere.

REFERENCES AND NOTES

- P. Bergveld, *IEEE Trans. Biomed. Eng.* **BME-19**, 70 (1970).
- J. Janata and R. J. Huber, in *Ion-Selective Electrodes in Analytical Chemistry*, H. Freiser, Ed. (Plenum, New York, 1980), pp. 107-174.
- J. N. Zemel, *Anal. Chem.* **47**, 255A (1975).
- G. F. Blackburn, in *Biosensors Fundamentals and Applications*, A. P. F. Turner, I. Karube, G. S. Wilson, Eds. (Oxford Univ. Press, Oxford, 1987), pp. 481-530.
- H. M. McConnell, J. W. Parce, D. G. Hafeman, *Electr. Soc. Abstr.* **87**, 2272 (1987).
- _____, *Proc. Electrochem. Soc.* **87**, 292 (1987).
- D. G. Hafeman, J. W. Parce, H. M. McConnell, *Proceedings of the 2nd International Meeting on Chemical Sensors*, J. L. Aucouturier et al., Eds. (Bordeaux, 1986), p. 69.
- For a general reference on semiconductor photoresponses, see S. N. Sze, *Physics of Semiconductor Devices* (Wiley, New York, 1981), pp. 362-430.
- L. Bousse, P. de Rooij, P. Bergveld, *IEEE Trans. Electr. Dev.* **ED-30**, 1263 (1983).
- Y. G. Vlasov, A. J. Bratov, V. P. Letavin, in *Ion-Selective Electrodes 3*, vol. 8 of the *Analytical Chemistry Symposium Series*, E. Pungor, Ed. (Elsevier, Amsterdam, 1981), pp. 387-397.
- F. Chauvet, A. Amari, A. Martinez, *Sensors Actuators* **6**, 255 (1984).
- M. T. Pham and W. Hoffmann, *ibid.* **5**, 217 (1984).
- L. Bousse and J. D. Meindl, *ACS Symp. Ser.* **323**, 79 (1986).
- U. Oesch, D. Ammann, W. Simon, *Clin. Chem.* **32**, 1448 (1986).
- R. L. Blakeley and B. J. Zerner, *J. Mol. Catal.* **23**, 263 (1984).
- W. U. de Alwis, B. S. Hill, B. I. Meiklejohn, G. S. Wilson, *Anal. Chem.* **59**, 2688 (1987).
- D. S. Wright, H. B. Halsall, W. R. Heineman, *ibid.* **58**, 2995 (1986).
- F. A. Armstrong, H. A. O. Hill, N. J. Walton, *Q. Rev. Biophys.* **18**, 261 (1986).
- L. Goldstein, M. Levy, L. Shemer, *Biotechnol. Bioeng.* **25**, 1485 (1963).
- We are greatly indebted to G. Pontis, J. Kercso, and L. Bousse for helpful discussions and technical assistance. Supported in part by the Army Research Office and Defense Advanced Research Projects Agency.

8 February 1988; accepted 20 April 1988

Crystal Structure of Hexaazaoctadecahydrocoronene Dication $[\text{HAOC}]^{2+}$, a Singlet Benzene Dication

JOEL S. MILLER, DAVID A. DIXON, JOSEPH C. CALABRESE

The structures of hexaazaoctadecahydrocoronene, $[\text{HAOC}]^n$ ($n = 0, +2$), have been determined by single-crystal x-ray diffraction. Although HAOC is aromatic, its dication has a localized structure that is based upon Jahn-Teller-distorted cyanine/*p*-phenylenediammonium fragments. The structure is consistent with the singlet ground state as determined by magnetic susceptibility and contrasts with the simplest Hückel expectation of a triplet ground state.

THE MCCONNELL CONJECTURE (1, 2) has focused research toward the design and synthesis of stable organic molecules with triplet ground states in order to prepare a molecular/organic ferromagnet (3-6). Recently this goal has been achieved with the characterization of $[\text{Fe}^{\text{III}}(\text{C}_5\text{Me}_5)_2]^+[\text{TCNE}]^-$ (TCNE = tetracyanoethylene) as a bulk ferromagnet (3, 7). This mechanism requires stable radicals with a degenerate highest occupied molecular orbital (HOMO) that is not half-filled. Thus the radicals must possess a rotation axis of order $n \geq 3$ or have D_{2d} symmetry (2, 3, 8). Organic radicals such as the radical cations of HAOC (Fig. 1) or hexaamino-benzene (9) are examples of such materials. HAOC has been prepared (10, 11) and its dication, $[\text{HAOC}]^{2+}$, has been reported to have a ground-state triplet (6, 10, 12). Based upon these observations, we have prepared several salts of $[\text{HAOC}]^{2+}$ with donor-acceptor radical anions of the type that have been previously reported to stabilize ferromagnetic coupling as the $[\text{Fe}^{\text{III}}(\text{C}_5\text{Me}_5)_2]^+$ salt and observe only diamagnetic behavior (13). These results are surprising, as a simple Hückel model of the benzene π -system leads to the prediction of a triplet for the dication as previously reported for $[\text{C}_6\text{Cl}_6]^{2+}$ (14). Since we sought to understand the diamagnetic behavior and since these high-symmetry, low-ionization potential donors are of theoretical interest, we prepared $[\text{HAOC}]^n$ ($n = 0, 1+, 2+$) as crystalline solids, and we

report the structure and magnetic properties of $[\text{HAOC}]^n$ ($n = 0, 2+$).

We prepared HAOC from hexaamino-benzene via a modified literature route (5, 10, 11, 13) and studied its single-crystal x-ray diffraction (15). The colorless crystals possess inversion crystallographic symmetry, and the idealized molecule belongs to the D_{3d} point group. The $[\text{HAOC}]^{2+}$ cation was prepared by oxidation with Ag^+ , and the 1:2 salts with $[\text{BPh}_4]$ (Ph, phenyl), $[\text{BF}_4]^-$, and $[\text{PF}_6]^-$ have been isolated as stable crystalline solids. The red crystals of $[\text{HAOC}]^{2+}$ as either the $[\text{BF}_4]^-$ (16) or $[\text{PF}_6]^-$ (17) salts have inversion crystallographic symmetry, and the idealized dication belongs to the C_{2h} point group. The dications are isolated from each other, as there are no intermolecular interactions less than 3.5 Å and the stacking is such that the benzene rings do not directly overlap. The average bond distances for HAOC and $[\text{HAOC}]^{2+}$ are listed in Table 1.

Cyclic voltammetry of HAOC showed that it has four reversible one-electron oxidations at -0.44, +0.06, +0.52, and +0.92 V (± 0.01 V) versus a standard calomel electrode (MeCN solvent) for the 0/1+, 1+/2+, 2+/3+, and 3+/4+ redox couples, respectively (13). The differences between potentials are comparable to previously reported values, although the absolute values deviate with those previously reported by +0.33 \pm 0.03 V (10).

The structures of HAOC and $[\text{HAOC}]^{2+}$ have the common feature of an approximately planar C_6N_6 moiety. The structure of HAOC has an aromatic benzene ring. Upon oxidation to the dication, the a and b C-C

Central Research and Development Department, Experimental Station E328, E. I. du Pont de Nemours & Company, Inc., Wilmington, DE 19898.

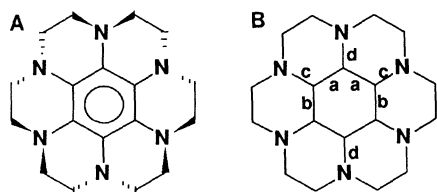
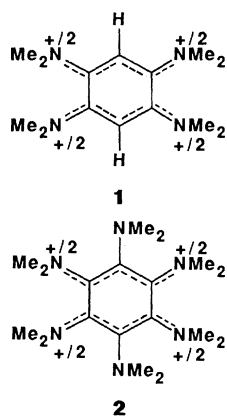


Fig. 1. Schematics of HAOC showing (A) geometry and (B) bond designations.

as well as the *c* and *d* C–N bond distances (Fig. 1B) become inequivalent, and a pair of localized cyanine/*p*-phenylenediammonium structure fragments are evident (Fig. 2).

The important valence bond structures (18) for $[\text{HAOC}]^{2+}$ are shown in Fig. 3, where the former pair of structures average to give the observed coupled cyanine structure. Were the latter to contribute equally, an averaged structure would be observed in the solid. Thus the 1E state for the cation derived from the D_{3d} geometry of the parent molecule undergoes a stabilizing Jahn-Teller distortion to yield the observed C_{2h} structure with a 1A_g ground state. A similar type of distortion has recently been reported for the dication salt of 1,2,4,5-tetrakis(dimethylamino)benzene, **1** (19), and hexakis(dimethylamino)benzene, **2** (20), although the C_6 rings of these molecules are non-planar.



The magnetic susceptibilities of $[\text{HAOC}]^n$ ($n = 0, 2+$) in the solid state were determined by the Faraday method. Both the neutral compound and the salts of the dication were diamagnetic and in the solid state. HAOC exhibited a diamagnetic susceptibility of $-190 \mu\text{emu/mol}$ at room temperature, which agrees well with the value of $-210 \mu\text{emu/mol}$ calculated from the Pascal constants. The temperature-independent susceptibilities of the $[\text{BF}_4]^-$ and $[\text{PF}_6]^-$ salts of $[\text{HAOC}]^{2+}$ were -228 and $-277 \mu\text{emu/mol}$, respectively. Sharp, multiplet-rich nuclear magnetic resonance (NMR) spectra consistent with the diamagnetic behavior were also observed. Previously the $[\text{HAOC}]^{2+}$ ion was reported to be a

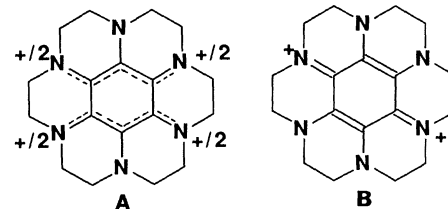
ground-state triplet (6, 10, 12); however, we observed temperature-independent diamagnetic behavior with a small (0.4%) $S = 1/2$ Curie contribution below 10 K (where S is the spin state). This is attributed to $[\text{HAOC}]^{\cdot+}$ impurities, which were observed by electron paramagnetic resonance (EPR) and have a characteristic EPR signal. The doublet impurity was observed at a $\sim 1\%$ level in CH_2Cl_2 or MeCN in fluid or frozen solutions (13).

Ab initio molecular orbital calculations on HAOC and $[\text{HAOC}]^{2+}$ were performed (21) with the STO-3G (22) minimal basis set (144 orbitals). The geometries were gradient optimized (23, 24) for the singlet state. Force fields were calculated analytically (25) and MP-2 correlation energy corrections were also calculated (26, 27).

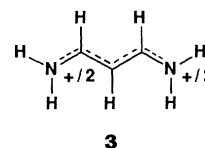
The optimized structure for HAOC has D_{3d} symmetry, and the average bond distances are listed in Table 1. The calculated C–C bond lengths in the benzene ring are in excellent agreement with the experimental values. The remaining calculated bond lengths are 0.03 to 0.04 Å too long. The benzenoid carbon atoms are slightly positive (+0.06 e) and the nitrogen atoms are quite negative (−0.28 e). The e_g HOMO (4.6 eV) is degenerate and is essentially equally localized on the benzenoid carbons and on the nitrogens. These results show that oxidation of HAOC should lead to a loss of electrons from the nitrogen lone pairs as well as from the degenerate benzene orbital.

The calculated structure of the singlet dication shows a significant deviation from the pseudo-sixfold symmetry of the benzene moiety and the nitrogen atoms found in HAOC. We started from the crystal coordinates and optimized a structure of approximate C_{2h} symmetry. This structure, **A**, has one negative direction of curvature at the Hartree-Fock level. Following this distortion, we reoptimized the structure to obtain the structure **B** with S_2 symmetry. Structure **B** is a true minimum on the Hartree-Fock

surface and has an energy of 1.8 kcal/mol less than that of structure **A** at the Hartree-Fock level. This situation reverses at the MP-2 correlated level and the energy of **A** is 5.4 kcal/mol less than that of **B**.



Structure **A** can best be described as two singlet cyanine dye cation moieties connected by C–C single bonds. This structure corresponds to a Jahn-Teller distortion. The agreement between structure **A** and the experimental structure is very good. The calculated value for C–C bond distance *a* is in excellent agreement with the experimental value. The distance *b* is consistent with a single C–C bond and is calculated to be 0.05 Å longer than that observed and that would be expected for an sp^2 - sp^2 C–C single bond. The calculated C–N bond distances *c* in $[\text{HAOC}]^{2+}$ are 0.1 Å shorter than the calculated value in HAOC and are only 0.02 Å longer than the experimental values in $[\text{HAOC}]^{2+}$. The remaining two C–N bond lengths *d* are calculated to lengthen slightly in $[\text{HAOC}]^{2+}$ as compared with HAOC. Thus they remain as single C–N bonds. The calculated bond distances *r* (27) for the model cyanine **3** are $r(\text{C–C}) = 1.389 \text{ \AA}$ and $r(\text{C–N}) = 1.337 \text{ \AA}$, which are in excellent agreement with our calculated values for $[\text{HAOC}]^{2+}$



The calculated structure **B** can be described as a *p*-phenylenediamine system or equivalently as one of the set of localized valence bond structures of the cyanine sys-

Table 1. Average bond lengths (Å) for $[\text{HAOC}]^n$ ($n = 0, 2+$). The positions of bonds *a*, *b*, *c*, and *d* are shown in Fig. 1B. The estimated standard deviations are shown in parentheses and are the variation in the last digit. Abbreviations: Obs, observed; Calc, calculated; and Avg, average.

Bond	Molecule/cation						
	HAOC	HAOC	$[\text{HAOC}]^{2+}$	$[\text{HAOC}]^{2+}$	$[\text{HAOC}]^{2+}$	$[\text{HAOC}]^{2+}$	
	(Obs)	(Calc)	$[\text{BF}_4]^-$ (Obs)	$[\text{PF}_6]^-$ (Obs)	(Avg) (Obs)	A _{Calc}	B _{Calc}
<i>a</i>	1.397*	1.401	1.397†	1.390‡	1.3935	1.401§	1.491
<i>b</i>	1.397*	1.401	1.475 (4)	1.478 (4)	1.4765	1.522	1.353
<i>c</i>	1.416	1.453	1.333¶	1.331#	1.332	1.349**	1.423
<i>d</i>	1.416	1.453	1.411 (3)	1.415 (3)	1.413	1.458	1.318

*Averaged from 1.388 (5), 1.399 (6), and 1.405 (5). †Averaged from 1.409 (4) and 1.384 (4). ‡Averaged from 1.384 (4) and 1.396 (4). §Averaged from 1.388 and 1.414. ¶Averaged from 1.428 (5), 1.405 (5), and 1.414 (5). #Averaged from 1.325 (4) and 1.340 (3). **Averaged from 1.327 (3) and 1.335 (3). **Averaged from 1.356 and 1.341.

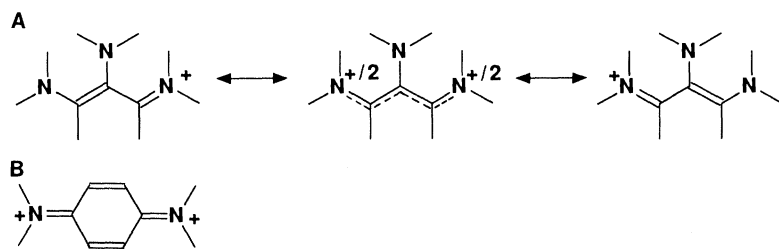


Fig. 2. Structures of (A) cyanine dyes and (B) *N,N,N',N'*-tetramethyl-*p*-phenylenediammonium dication.

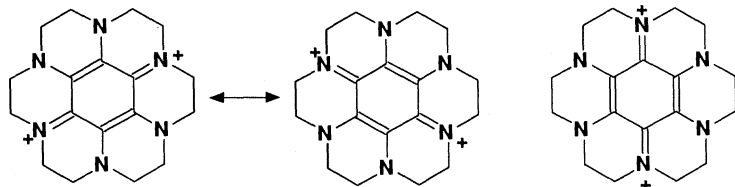
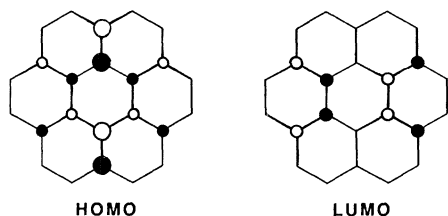


Fig. 3. Important valence bond structures for [HAOC]²⁺.

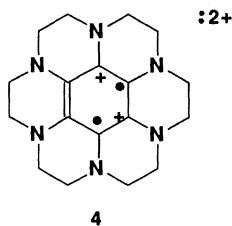
tems and represents the other Jahn-Teller distortion. The cyanine structures are localized with maximal charge separation. In contrast to structure A, there are two short C–C bonds **b** and C–N bonds **d** that have double-bond lengths and four long C–C bonds **a** and C–N bonds **c** that are like single bonds. The four C–N bonds **c** are somewhat short compared with the C–N bond lengths in HAOC.

The HOMO and lowest unoccupied molecular orbital (LUMO) for the lowest energy structure at the MP-2 level (that is, the experimental structure) are derived from the degenerate e_g HAOC HOMO (like the e_{1g} benzene HOMO) and are significantly split in energy. They are shown schematically below with solid balls representing negative phase and open balls representing positive phase. The HOMO of [HAOC]²⁺ has at least as much nitrogen character as benzenoid carbon character, as was determined for HAOC. The shape of the HOMO is consistent with the distortion leading to the coupled delocalized cyanine structures separated by single bonds. The largest density in the HOMO is found on the nitrogen atoms that are not part of the cyanine structures. The LUMO is an antibonding orbital between the C–N bonds in the cyanines. These orbitals are consistent with the expected Jahn-Teller distortions.



The experimental results confirm that a dication based upon an aromatic C₆ ring can be stabilized by six nitrogens as a singlet.

The dication has a closed shell configuration that is best described by a pair of cyanine fragments and has reasonable chemical stability in the ambient. The magnetic and structural studies are consistent with the absence of a [HAOC]²⁺ triplet, **4** (10). Additionally, our molecular orbital computational studies are consistent with these observations and suggest that the dications of hexaaza-substituted benzenes can be closed shell.



The McConnell mechanism for stabilization of ferromagnetic coupling, but not bulk ferromagnetic behavior, in a molecular solid requires the configurational mixing of a ground state possessing a doubly degenerate orbital with the lowest lying charge-transfer excited state with spin conservation. Thus a stable triplet species is anticipated to be a necessary component in the design of a molecular/organic ferromagnet (3, 29), and singlet dications such as [HAOC]²⁺ are inappropriate (30). Stabilization of the triplet ground state thus requires a lack of dominance by singlet resonance structures, so that the energy of the degenerate singlet state is not lowered by a large amount by the Jahn-Teller distortion or equivalently by a negative value for the electron exchange integral for the diradical electrons (31, 32).

REFERENCES AND NOTES

1. H. M. McConnell, *Proc. R. A. Welch Found. Chem. Res.* **11**, 144 (1967).

2. J. S. Miller and A. J. Epstein, *J. Am. Chem. Soc.* **109**, 3850 (1987).
3. ———, W. M. Reiff, *Chem. Rev.* **88**, 201 (1988); *NATO Adv. Studies Ser. B* **168**, 159 (1987); *Acc. Chem. Res.* **21**, 114 (1988); *Science* **240**, 40 (1988).
4. R. Breslow, *Pure Appl. Chem.* **54**, 927 (1982).
5. ———, B. Jaun, R. Q. Klutz, C.-Z. Xia, *Tetrahedron* **38**, 863 (1982).
6. R. Breslow, *Mol. Cryst. Liq. Cryst.* **125**, 261 (1985).
7. J. S. Miller *et al.*, *J. Am. Chem. Soc.* **109**, 769 (1987).
8. This assumes that the virtual charge transfer involves only the highest energy partially occupied molecular orbital (POMO). Circumstances where virtual excitation from a lower lying filled (or to a higher lying unfilled) orbital dominate the admixing exciting state are conceivable, and the orbital degeneracy and symmetry restrictions are relaxed. For example, [Cr¹(C₆Me₆)₂]⁺[TCNE]⁻ has a nondegenerate POMO ground-state electronic configuration, and preliminary susceptibility data can be fit by the Curie-Weiss expression with a temperature $\theta = +12$ K, which suggests that ferromagnetic interactions dominate; J. S. Miller, D. M. O'Hare, A. Chackraborty, A. J. Epstein, unpublished results.
9. D. A. Dixon, J. C. Calabrese, J. S. Miller, unpublished results.
10. R. Breslow, P. Maslak, J. S. Thomaidis, *J. Am. Chem. Soc.* **106**, 6453 (1984).
11. B. Kohne, K. Praefcke, A. Reichmann, *Chem. Ztg.* **109**, 17 (1985).
12. T. J. LePage and R. Breslow, *J. Am. Chem. Soc.* **109**, 6412 (1987).
13. J. S. Miller *et al.*, unpublished results.
14. E. Wasserman, R. S. Hutton, V. J. Kuck, E. A. Chandross, *J. Am. Chem. Soc.* **95**, 1965 (1974).
15. The following crystallographic results at -70°C were obtained: space group $P2_1/c$; $a = 9.784$ (2) Å; $b = 9.384$ (4) Å; $c = 9.614$ (8) Å; $\beta = 117.54$ (3)°; $V = 782.7$ Å³; $Z = 2$; and $R_w = 5.3\%$, where a , b , and c are the length and β is the angle that define the unit cell, V the volume of the unit cell, Z the number of molecules in the unit cell, and R_w , the weighted agreement factor; estimated standard deviations are expressed parenthetically as the variation in the last digit.
16. The following crystallographic results at -70°C were obtained: space group $P2_1/m$; $a = 6.604$ (1) Å; $b = 10.929$ (2) Å; $c = 14.255$ (3) Å; $\beta = 91.33$ (1)°; $V = 1028.6$ Å³; $Z = 2$; and $R_w = 4.3\%$.
17. The following crystallographic results at -70°C were obtained: space group $P1$; $a = 6.666$ (2) Å; $b = 8.915$ (1) Å; $c = 10.632$ (2) Å; $\alpha = 100.45$ (1)°, $\beta = 108.82$ (2)°, $\gamma = 105.09$ (1)°; $V = 577.0$ Å³; $Z = 2$; and $R_w = 4.3\%$; α , β , and γ are angles that define the unit cell.
18. Throughout the remainder of the manuscript only one of several resonance structures are depicted.
19. K. Elbl, C. Krieger, H. A. Staab, *Angew. Chem. Int. Ed. Engl.* **25**, 1023 (1986); *Angew. Chem.* **98**, 1024 (1986).
20. J. M. Chance, B. Kahr, A. B. Buda, J. P. Toscano, K. Mislow, unpublished results.
21. The calculations were performed with the program GRADSCF on a CRAY-XMP/24 computer. GRADSCF is an ab initio gradient program system designed and written by A. Komornicki at Polyatomics Research, Mountain View, CA.
22. The STO-3G basis set has 1s, 2s, and three 2p functions on carbon, nitrogen, and oxygen atoms. These basis sets are formed by contracting three Gaussian functions for each basis function as described by W. J. Hehre, R. F. Stewart and J. A. Pople [*J. Chem. Phys.* **51**, 2657 (1969)].
23. P. Pula, in *Applications of Electronic Structure Theory*, H. F. Schaefer III, Ed. (Plenum, New York, 1977), chap. 4.
24. A. Komornicki, K. Ishida, K. Morokuma, R. Ditchfield, M. Conrad, *Chem. Phys. Lett.* **45**, 595 (1977).
25. H. F. King and A. Komornicki, *J. Chem. Phys.* **84**, 5645 (1986).
26. C. Moller and M. S. Plesset, *Phys. Rev.* **46**, 618 (1934).
27. J. A. Pople, J. S. Binkley, R. Seeger, *Int. J. Quantum Chem. Symp.* **10**, 1 (1976).
28. D. A. Dixon and D. F. Eaton, unpublished results.
29. A stable triplet may not be necessary for an organic ferromagnet; two doublets with a virtually accessible

triplet capable of admixing with ground state, as observed for $[\text{Fe}^{\text{III}}(\text{C}_5\text{Me}_5)_2]^+[\text{TCNE}]^-$, should suffice.

30. Other hexasubstituted benzene dications may also have singlet ground states, and their structures and magnetic properties should be investigated.
31. Elimination of "pseudo-sixfold" symmetry may stabilize the triplet ground state.
32. J. E. Wertz and J. R. Bolton, *Electron Spin Resonance* (Chapman & Hall, New York, 1986), p. 244 and section 10-11.

33. We are indebted to P. J. Krusic and M. D. Ward for providing EPR and electrochemical data, respectively, and for stimulating discussions with them and E. Wasserman. We appreciate the synthetic assistance of C. Vazquez and D. Wipf, as well as the x-ray diffraction assistance of W. Marshall and Faraday susceptibility data taken by R. S. McLean. We also thank K. Mislow for kindly providing a preprint prior to publication.

4 March 1988; accepted 1 April 1988

Virus-Like Particles and a Spider Mite Intimately Associated with a New Disease of Barley

NANCY L. ROBERTSON AND THOMAS W. CARROLL

The malting barley-producing regions in Montana and Canada are threatened with a new virus-like barley disease that appears to be etiologically novel. Ultrathin sections of diseased tissue contained enveloped, filamentous virus-like particles that measured 64 nanometers by 126 to 4000 nanometers. These lengths are unique for plant viruses. Unexpectedly, the spider mite, *Petrobia latens*, which has never been reported to be a vector of a pathogen, was found to transmit the causal agent from diseased plants to healthy barley, while noninfective mites failed to do so unless they were allowed prior access to diseased tissue.

IN 1982, A DISEASE OF BARLEY (*Hordeum vulgare* L.) was discovered in one barley field in the malting barley-producing area of north central Montana. In 1983 and 1984, the disease was also present in other barley fields as distant as 24 km. In 1985, and again in 1986 and 1987, the disease reached epidemic levels in that area and was also identified in five other contiguous counties. Malting barley producers reported that the disease was causing yield losses and preventing them from meeting malting standards.

When ultrathin sections and crude extracts of diseased leaves (1) were examined (Zeiss EM 10 CA electron microscope), long filaments about 64 nm in diameter (2) were found that met one size criterion for virus particles (3, 4). Many of the particles had extraordinary lengths, with some over 4000 nm in ultrathin sections. Such lengths for intact virus particles have not previously been reported for plant viruses but have been documented for viruses in animals (5) and insects (6). Inasmuch as these virus-like particles (VLPs) appeared only in diseased tissue and morphologically resembled some virus particles, we hypothesized that they were the causal agent of the disease and conducted tests to determine their possible modes of transmission.

The barley seed we collected in 1983 from

diseased field plants were sown in the greenhouse and produced no diseased plants (7). Healthy barley seedlings did not become diseased in the greenhouse after mechanical inoculation of triturated diseased leaves (7). In another greenhouse test, healthy barley seedlings grown in field soil from a diseased site failed to develop disease symptoms (7). From 1983 through 1985, we conducted extensive transmission tests with aphid, leafhopper, and thrips species (many of which are known to transmit plant viruses) (8) collected from fields of diseased barley. Again, there was no transmission when these species were separately allowed to feed on healthy indicator test seedlings in the greenhouse (7).

However, by 1986, infestations of the brown wheat mite, *Petrobia latens* Muller (Acari: Tetranychidae), were observed to occur on seedlings in fields of barley with subsequent development of the disease. Although brown wheat mite infestations appear sporadically in cereal crops throughout the world (9), the mite has never been associated with the transmission of a plant pathogen. To test the hypothesis that *P. latens* was a vector for the causal agent of this disease, we collected immature and adult stages of the mites (10, 11) from fields of diseased Klages barley in June 1986 by tapping infested leaves, which caused the mites to fall onto a sheet of white paper (12). We then allowed the mite population to feed on caged healthy barley seedlings for 2 months in the greenhouse (13). Plants

were observed for symptoms, and ultrathin sections of leaf samples were examined to confirm the presence or absence of the VLPs.

In June 1987, we collected mites from the same site of diseased Klages barley and obtained another set of mites from a contiguous field of Lew spring wheat, which had only a trace of the disease. These two populations of mites and their progeny were maintained separately in two cages on barley seedlings. Four consecutive sets of seedlings were exposed to those mites in the cages every 3 weeks. Each set contained 16 Dicktoo barley seedlings, which were initially exposed to the mites at the one-leaf stage (four plants per 15-cm-diameter pot). Approximately 400 mites were placed in each of the cages in the beginning of the experiments. At the end of each cycle, mites were aspirated or gently tapped from the infested seedlings and placed onto the new set of seedlings (14). We then fumigated these plants for 2 hours with Vapona (dichlorvos) pesticide before transplanting each plant into pots 20 cm in diameter; the plants were grown and observed in the greenhouse for at least eight more weeks under a 16-hour-per-day photoperiod at temperatures between 20° and 27°C. All plants were assayed for the presence or absence of the VLPs by the leaf extract procedure.

At the end of the fourth cycle, we removed 44 mites from the population that originated from the wheat site and divided them into two groups. In parallel transmission tests, one group of the mites was placed on detached diseased leaves and the other

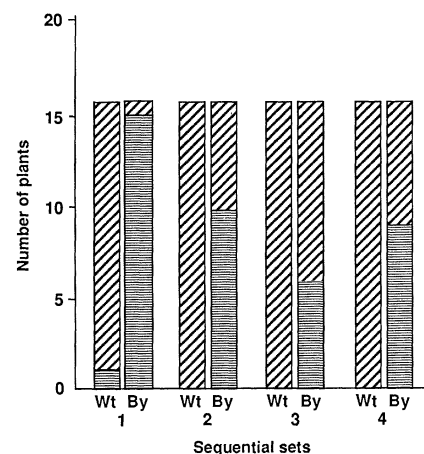


Fig. 1. Effects of exposing healthy barley seedlings to mites that originated from fields of wheat (Wt) or barley (By). Mites derived from healthy-appearing wheat produced only one symptomatic plant in the first set of plants, whereas mites derived from a field of diseased barley were associated with symptomatic plants in every set of plants exposed to the mites (hatched, nonsymptomatic; horizontal lines, symptomatic). Only diseased tissue contained the associated VLPs (18).